Tumor and Stem Cell Biology

Cancer Research

IL4 Primes the Dynamics of Breast Cancer Progression via DUSP4 Inhibition

Miriam Gaggianesi[1], Alice Turdo[1], Aurora Chinnici[1], Elisa Lipari[1], Tiziana Apuzzo[1], Antonina Benfante[1], Isabella Sperduti[2], Simone Di Franco[1], Serena Meraviglia[3,4], Elena Lo Presti[3], Francesco Dieli[3,4], Valentina Caputo[5], Gabriella Militello[6], Salvatore Vieni[1], Giorgio Stassi[1], and Matilde Todaro[3,5]

Abstract

The tumor microenvironment supplies proinflammatory cytokines favoring a permissive milieu for cancer cell growth and invasive behavior. Here we show how breast cancer progression is facilitated by IL4 secreted by adipose tissue and estrogen receptor–positive and triple-negative breast cancer cell types. Blocking autocrine and paracrine IL4 signaling with the IL4Rα antagonist IL4DM compromised breast cancer cell proliferation, invasion, and tumor growth by downregulating MAPK pathway activity. IL4DM reduced numbers of $CD44^+/CD24^-$ cancer stem-like cells and elevated expression of the dual specificity phosphatase DUSP4 by inhibiting NF-κB. Enforced expression of DUSP4 drove conversion of metastatic cells to nonmetastatic cells. Mechanistically, RNAi-mediated attenuation of DUSP4 activated the ERK and p38 MAPK pathways, increased stem-like properties, and spawned metastatic capacity. Targeting IL4 signaling sensitized breast cancer cells to anticancer therapy and strengthened immune responses by enhancing the number of IFNγ-positive CTLs. Our results showed the role of IL4 in promoting breast cancer aggressiveness and how its targeting may improve the efficacy of current therapies. *Cancer Res; 77(12); 3268–79. ©2017 AACR.*

Introduction

Despite the advent of efficacious treatment of primary breast cancer lesions, metastatic disease is poorly sensitive to the common therapeutic regimens (1).

Adipose tissue is the most abundant constituent of the breast cancer microenvironment and is mainly composed of mature adipocytes, preadipocytes, and adipose-derived stem cells (ADSC; ref. 2). Obesity and overweight have recently been suggested as being meaningful risk factors for the development of breast cancer and its therapy resistance (3). Indeed, compelling evidence shows that paracrine signals, provided by the adipose tissue and surrounding cancer cells, contribute to tumorigenesis and cancer progression (2, 4). Secreted protumorigenic cytokines and hormones feed breast cancer cells regardless of their hormone status and are also responsible for the acquisition of an aggressive cell phenotype (5).

Furthermore, we have identified autocrine and paracrine production of IL4 as a survival signal and tool to protect colorectal cancer cells from anticancer therapy, through the upregulation of antiapoptotic molecules (6, 7). Indeed, IL4 is a pleiotropic cytokine secreted by fibroblasts, immune, adipose, and a wide range of epithelial cells, including breast cancer cells (8). IL4 cognate receptors comprise two types: (i) type I IL4R (IL4RI) and (ii) type II IL4R (IL4RII). The first is mainly present on immune cells and characterized by the heterodimerization of the IL4Rα and the common γ-chain subunits. IL4RII, on the other hand, is present on nonhematopoietic cells and composed of IL4Rα and the IL13Rα1 subunits. IL4RII is expressed on the surface of many cancer cells and lacks intrinsic kinase activity, thus it requires further associated kinases for the initiation of signal transduction (8). Upon binding of IL4, the tyrosine kinases Jak1/2 and Tyk2 are indeed recruited on the transmembrane domain of IL4RII and mediate its phosphorylation, leading to the activation of PI3K/AKT, MAPK, and Jak/STAT6 downstream pathways (8).

In breast cancer, the secretion of the protumorigenic cytokines, IL6 and IL8, is controlled by the dual specificity phosphatase 4 (DUSP4; ref. 9). In physiologic conditions, the transcription of *DUSP4* is MEK-dependent and its expression in turn suppresses ERK, along with p38, JNK1, NF-κB, and Rb (9–12), ensuring a proper negative feedback control of cellular proliferative stimuli. DUSP4 is differentially expressed among luminal and basal breast cancers. Specifically, the most aggressive tumors hold DUSP4 under-expression, due to methylation events or genomic loss (9, 10).

It has been clearly demonstrated that a subpopulation of cancer cells, named tumor-initiating cells (TIC), is endowed with the capability of self-renewal and tumor initiation (13–16). Indeed, this cell compartment is refractory to the common anticancer drugs and responsible for recurrence (13–16).

[1]Department of Surgical, Oncological and Stomatological Sciences, University of Palermo, Palermo, Italy. [2]Regina Elena National Cancer Institute, Rome, Italy. [3]Central Laboratory of Advanced Diagnosis and Biomedical Research (CLADIBIOR), University of Palermo, Palermo, Italy. [4]Department of Biopathology and Biomedical Methodologies, University of Palermo, Palermo, Italy. [5]Department of DIBIMIS, University of Palermo, Palermo, Italy. [6]Department of Emergency, General Surgery and Organ Transplants, University of Palermo, Palermo, Italy.

Note: Supplementary data for this article are available at Cancer Research Online (http://cancerres.aacrjournals.org/).

M. Gaggianesi and A. Turdo contributed equally to this article.

Corresponding Author: Matilde Todaro, University of Palermo, Via del Vespro, 131, Palermo 90127, Italy. Phone: 390916552607; Fax: 390916553238; E-mail: matilde.todaro@gmail.com

doi: 10.1158/0008-5472.CAN-16-3126

Published OnlineFirst April 11, 2017; DOI: 10.1158/0008-5472.CAN-16-3126

An inflammatory microenvironment has been shown to favor the maintenance of the breast TICs and their invasive behavior (17, 18). However, insufficient data are available on the mechanisms regulating this phenomenon. Recently, it has been demonstrated that, in a syngeneic breast cancer mouse model, the IL4/IL4R interaction promotes metastatic spreading by activating the MAPK pathway (19).

Taken together, these findings suggest that IL4 may conceivably play a role in the progression of breast cancer and resistance to standard therapeutic regimens driven by TICs. In this study, we establish for the first time the molecular mechanisms elicited by IL4, which augment proliferation and invasiveness of breast cancer sphere cells (BCSC), notoriously largely composed of TICs (15). Blocking autocrine and paracrine IL4 signaling via the attenuation of the MAPK pathway, counteracts the protumorigenic effect of all the proinflammatory cytokines released by ADSCs. Moreover, we unveil that IL4 acts through NF-κB to lower DUSP4 expression levels.

Here, we emphasize the role of IL4 in the metastatic potential of BCSCs and its neutralization as a useful strategy for therapeutic intervention.

Materials and Methods

Tissue collection

Breast cancer tissues were collected at the Department of Surgical, Oncological and Stomatological Sciences (University of Palermo, Palermo, Italy), in accordance with the ethical standards of the Institutional Committee on Human Experimentation and their molecular subtypes. Breast cancer characterization was established using the following IHC markers (20): ER^+, $PR^{+/-}$, $HER2^-$, $Ki67^{low}$ (luminal A); ER^+, $PR^{+/-}$, $HER2^-$, $Ki67^{high}$ or ER^+, $PR^{+/-}$, $HER2^+$ (luminal B); ER^-, PR^-, $HER2^+$ (HER2 amplified); ER^-, PR^-, $HER2^-$ (triple negative breast cancer, TNBC; Table 1). Cancer staging was determined according to the 7th Edition AJCC classification of malignant tumors.

Isolation and culture of cancer cells

Breast cancer tissue was mechanically and enzymatically digested using collagenase (1.5 mg/mL; Gibco) and hyaluronidase (20 mg/mL; Sigma Aldrich) in DMEM and shaken for 1 hour at 37°C. The recovered cell suspension was plated in ultra-low attachment flasks in serum-free medium (SFM) supplemented with basic fibroblast growth factor (bFGF; 10 ng/mL; PeproTech) and EGF (20 ng/mL; PeproTech), as previously described (21, 22). SFM allows breast cancer cells to propagate as sphere structures, which are enriched in cells that harbor stem-like and tumor-initiating properties (6, 13, 15). We used ER^+-BCSCs derived from luminal B patients #4 and #18 and TN-BCSCs, derived from TNBC patients #10 and #30 (Table 1) for all the experiments performed. BCSCs and their relative tumor tissues were authenticated using a highly informative short tandem repeat (STR) system (GlobalFiler STR Kit; Applied Biosystems) and then sequenced using the ABIPRISM 3130 genetic analyzer (Applied Biosystems). CD90 staining was used to exclude the presence of stromal cells within the ER^+- and TN-BCSC compartment. Human ADSCs were purchased from STEMPRO and cultured for less than six passages according to manufacturer's instructions. MCF7 cell line was purchased from CLS cell line service in July 2013, authenticated from the cell bank by DNA profiling (STR analysis), and maintained in 10% FBS DMEM. Cells, expanded for two passages after receipt, were then frozen and used within 6 months after thawing. SUM159 cell line was kindly provided by Prof. Max Wicha (University of Michigan, Ann Arbor, MI) and authenticated in our laboratory by STR as described above. SUM159 cells were cultured in Ham F-12, 5% FBS, hydrocortisone (1 μg/mL; Sigma), insulin (5 μg/mL; Sigma-Aldrich). Cells were routinely tested for mycoplasma infection with MycoAlert PLUS Mycoplasma Detection Kit (Lonza), revealed using Infinite F500 (Tecan).

Both BCSCs and established breast cancer cell lines were exposed to ADSC conditioned medium (ADSC-CM), IL4 (20 ng/mL; PeproTech), and the IL4Rα antagonist (IL4DM; 15 μg/mL), kindly donated by Apogenix. IL4DM was administered for a total of 72 hours. All treatments were replenished every 48 hours.

Withaferin A (Wit A, 2 μmol/L, Tocris) and 5-aminosalicylic acid (5-ASA, 26 mmol/L; Sigma-Aldrich) were used as NF-κB inhibitors and added 1 hour and 30 minutes before IL4 treatment, respectively.

For the cell viability assay, BCSCs were exposed to fulvestrant (1 μmol/L; Selleckchem), docetaxel (100 nmol/L; Selleckchem) or BKM120 (5 μmol/L; Selleckchem). BCSCs were exposed to IFNγ (100 ng/mL; Novus Biologicals), as positive control for PD-L1 expression, for 4 and 24 hours.

To evaluate the expression of PD-1 or IFNγ in gated $CD8^+$ T cells, 5×10^5 PBMCs/mL were activated (Activated) for 4 days in 24-well plates coated with purified anti-human CD3ε (OKT3, IgG2a; Biolegend), anti-human CD28 (CD28.2, IgG1κ; Biolegend), and in presence of human rIL2 (100 IU/mL Proleukin; Novartis Pharmaceuticals) in 10% FBS RPMI. Activated cells were then treated, for additional 4 days, with medium (medium), IL4, IL4DM alone, or in combination with IL4 (IL4+IL4DM). Prior flow cytometry analysis, for the intracellular staining of cytokines, untreated and treated activated cells were cultured in presence of PMA (20 ng/mL; BD Biosciences) and ionomycin (1 μmol/L; BD Biosciences) for 4 hours and for the last 3 hours in combination with monensin (2 μmol/L; Sigma-Aldrich), for blocking cellular protein transport.

CM production and Luminex cytokine quantification

CM from ADSCs (ADSCs-CM), ER^+-BCSCs (ER^+-CM) and TN-BCSCs (TN-CM) were obtained from cells plated at 70% confluence and cultured in SFM for 48 hours. CM was filtered through a 0.22-μm filter to eliminate cell debris.

Table 1. Description of breast cancer clinical features

Patient	Grading	ER	PR	*HER2* amplification	Ki67	Clinical receptor subtype	Sphere formation	Xenograft formation
#4	G2	+	+	Yes	>10%	Luminal B	Yes	Yes
#10	G2	−	−	No	>10%	TNBC	Yes	Yes
#18	G2	+	+	Yes	>10%	Luminal B	Yes	Yes
#30	G3	−	−	No	>10%	TNBC	Yes	Yes

Abbreviations: ER, estrogen receptor; PR, progesterone receptor.

Published OnlineFirst April 11, 2017; DOI: 10.1158/0008-5472.CAN-16-3126

Quantification of cytokine production was assessed by using multiplex Bio-Plex Pro Assays (Human Cytokine 21 and 27-plex Assay; Bio-Rad). Raw data (mean fluorescence intensity) were analyzed by Bio-Plex Software (Bio-Rad).

Cell motility and invasion assay

A total of 1×10^3 BCSCs were plated into 6-well attachment plates in DMEM with 10% FBS to allow cell attachment. The spreading of cells, which were treated with medium alone, ADSC-CM, or IL4 in presence of 5% FBS, was determined by phase contrast microscopy at 12 hours.

A total of 2×10^3 breast cancer cells, treated with IL4DM for 24 hours and subsequently exposed to ADSCs-CM or IL4 for another 48 hours in SFM, were plated onto growth factor–reduced matrigel (BD Biosciences)-coated transwell of 8-μm pore size. SFM in presence of 10% human serum AB was used as a chemoattractant in the bottom part of the chamber (600 μL/well). Cells invading Matrigel were monitored and counted using an optical microscope for up to 48 hours.

Cell viability

Cell viability was performed using the CellTiter-Glo Luminescent Cell Viability Assay Kit (Promega) according to the manufacturer's instruction. Cell proliferation was assessed using CellTiter 96 AQueous One Solution cell proliferation assay (MTS) according to the manufacturer's instruction. Detection of both luminescence and absorbance was measured by using Infinite F500 (Tecan).

Stem cell frequency and colony-forming efficiency

BCSCs were plated at a concentration of a single cell per well. Wells containing more than three cells were excluded. The stem cell frequency was statistically evaluated after 3 weeks by using ELDA analysis program (23). For the colony-forming assay, 500 dissociated BCSCs were mixed with 0.3% agarose (SeaPlaque Agarose Lonza) in SFM and seeded onto a layer of 0.4% agarose. After 20 days, colonies were stained with 0.01% crystal violet in 1% methanol. Colonies were first distinguished on the basis of their size: micro < 30 μm; small 30–60 μm; medium 60–90 μm; and large >90 μm and then counted using ImageJ software.

Animals and tumor models

Mice experiments were performed according to the ARRIVE and animal care committee guidelines of the University of Palermo. A total of 4×10^3 BCSCs, treated with medium alone or IL4 for 24 hours, were suspended in 100 μL of SFM 1:1 Matrigel (BD Biosciences) and injected subcutaneously into 6-week-old female NOD/SCID mice (Charles River Laboratories). After 1 week, mice were intraperitoneally treated with vehicle (PBS) or IL4DM (3 mg/kg) 5 days/week for 10 weeks (6, 24). One week after the end of treatment, at 12 weeks, mice were sacrificed following IACUC guidelines and tumor xenografts were collected. Tumor growth was monitored weekly with an electronic caliper. Tumor volume was calculated using the formula: largest diameter $\times$ (smallest diameter)$^2 \times \pi/6$. For tail vein experiments, 1.5×10^5 luciferase (LUC)-transduced BCSCs (Supplementary Information) were suspended in 30 μL of PBS and injected into 6-week-old female NOD/SCID mice. After injection of VivoGlo Luciferin (150 mg/kg; Promega), *in vivo* cell spreading was monitored by the detection of bioluminescence intensity using a Photon IMAGER (Biospace Lab), for up to 9 weeks. The photon count (photons/s/sr, photons per second per steradian), emitted by mice metastasis, was calculated by using M3 Vision (Biospace Lab). Mice were sacrificed when lesions reached 4×10^3 photons/s/sr, corresponding to a ≤ 0.5 cm^2 tumor area, and liver and lungs were analyzed *ex vivo* to detect metastasis formation.

Flow cytometry

ER$^+$- and TN-BCSCs were washed twice in PBS and stained at 4°C with purified CD44-PE (G44-26, mouse IgG2b; BD Biosciences), CD24-APC (ML5, mouse IgG2a; R&D Systems), CD10-APC (97C5, mouse IgG1; Miltenyi Biotec), MUC1-PE (604804, mouse IgG2b; R&D Systems), CD49f-APC (GoH3, rat IgG2a; Miltenyi Biotec), EPCAM-PerCP (EBA-1, mouse IgG1; BD Biosciences), or CD90-PE-CF594 (5E10, IgG1κ; BD Biosciences) antibodies or corresponding IMC CD14-PE (MϕP9, IgG2b; BD Biosciences), CD4-APC (11830, IgG2a; R&D Systems), CD4-APC (REA623, IgG1; Miltenyi Biotec), CD8-PE (37006, IgG2b; R&D Systems), CD3-APC (BW264/56, IgG2a; Miltenyi Biotec), CD3-PERCP (SP34-2, IgG1; BD Biosciences), CD3-PE-CF594 (UCHT1, IgG1κ; BD Biosciences). Dead cells were excluded on the basis of light scatter and the uptake of 7-AAD (0.25 μg/L $\times$ 10^6 cells; BD Biosciences) detected in FL3 channel. Single cells were gated in FSC-A versus FSC-H dot plots. Samples were analyzed by FACSCanto II (BD Biosciences) or Accuri C6 (BD Biosciences) flow cytometer and data analyzed using FlowJo software (Tree Star).

PBMCs were incubated on ice with FcR blocking reagent (Miltenyi Biotec) and stained with CD3-PeCy7 (UCHT1, mouse IgG1κ; Biolegend), CD8-PE (RPA-T8, mouse IgG1κ; BD Biosciences), IFNγ-APC (B27, mouse IgG1κ; BD Biosciences), PD-1-FITC (EH12.2H7, mouse IgG1κ; Biolegend) antibodies or corresponding isotype matched controls (IMC), specifically APC mouse IgG1κ (MOPC-21; BD Biosciences) and FITC mouse IgG1κ (MOPC-21; Biolegend). For intracellular staining, cells were previously subjected to Cytofix/Cytoperm protocol following the manufacturer's instructions (BD Biosciences).

Western blot analysis

Cells were washed in ice-cold PBS and suspended in TPER Reagent (Pierce) in presence of NaCl (300 mmol/L; Sigma Aldrich), sodium orthovanadate (1 mmol/L; Sigma Aldrich), pefabloc (2 mmol/L; Roche), and proteinase inhibitor cocktail (5 μg/mL; Sigma Aldrich). Extracted proteins were loaded, separated by SDS-PAGE, and blotted onto nitrocellulose membranes (Hybond-C Extra, nitrocellulose; Amersham Biosciences). Membranes were blocked in 0.1% Tween 20 and 5% non-fat dry milk for 1 hour at room temperature and then exposed to DUSP4 (D9A5, rabbit IgG, Cell Signaling Technology), P-MEK (41G9, rabbit IgG, Cell Signaling Technology), MEK (rabbit polyclonal, Cell Signaling Technology), P-ERK (E-4, mouse IgG2a, Santa Cruz Biotechnology), ERK (rabbit polyclonal, Santa Cruz Biotechnology), RAS (27H5, rabbit IgG, Cell Signaling Technology), P-NF-κB (T.849.2, rabbit IgG, Thermo Fisher Scientific), NF-κB (112A1021, mouse IgG1κ; Thermo Fisher Scientific), P-P38 (D3F9, rabbit IgG; CST), P38 (rabbit polyclonal; Cell Signaling Technology), IL4Rα (25463.111, mouse IgG2a; R&D Systems), IL13Rα2 (goat polyclonal; R&D Systems), P-STAT6 (rabbit polyclonal; Cell Signaling Technology), STAT6 (rabbit polyclonal; Cell

Published OnlineFirst April 11, 2017; DOI: 10.1158/0008-5472.CAN-16-3126

Signaling Technology), PD-L1 (E1L3N, rabbit IgG; Cell Signaling Technology), or β-actin (8H10D10, mouse IgG2b; Cell Signaling Technology) antibody. Primary antibodies were revealed using anti-mouse or anti-rabbit HRP–conjugated (goat IgG; Thermo Fisher Scientific) and detected by a chemiluminescence imager (GE Healthcare).

Statistical analysis

Kaplan–Meier curves of relapse-free survival based on the gene expression ratio of IL4/DUSP4 in breast cancer patients were obtained by interrogating the PROGgeneV2 - Pan Cancer Prognostics Database-GSE10893-GPL887. Statistical analysis was calculated using ANOVA with Bonferroni *post test*. Significance was indicated as *P* values.

Results

ADSC-CM and IL4 promote expansion of BCSCs

The breast cancer microenvironment is abundantly composed of adipose tissue that constitutes a reservoir of protumorigenic molecules (25, 26). In the attempt to identify the main contributor to breast cancer cells expansion, we examined the composition of the CM from ADSCs (ADSCs-CM) as well as from ER^+- and TN-BCSCs (ER^+-CM and TN-CM, respectively). Several studies demonstrate that ADSCs promote proliferation and invasive capacity in breast cancer cells (27) and, interestingly, the maintenance of the breast TIC pool (28). Moreover, the use of ADSCs overcomes the difficulties experienced in the isolation and long-term culture of mature adipocytes from adipose tissue (4). ER^+- and TN-BCSCs, enriched with cells having stem-like properties, were obtained from surgical resection of breast cancers. ER^+-BCSCs were derived from patient #4 and #18, whereas TN-BCSCs from patient #10 and #30 (see Materials and Methods and Table 1), as described previously (22). ER^+ cells were positive for MUC1 and EPCAM, and expressed low levels of CD49f, whereas TN cells displayed epithelial-to-mesenchymal transition (EMT) markers such as CD10, CD49f, and VIMENTIN (Supplementary Fig. S1A and S1B).

Exploring the levels of a panel of cytokines across the CMs of ADSCs and ER^+- and TN-BCSCs, we detected a higher secretion of proinflammatory and protumorigenic cytokines in CMs of ADSCs and TN-BCSCs. These data suggest that TN-, as opposed to ER^+-BCSCs, support the generation of an inflammatory microenvironment, linked to enhanced tumorigenic features (Fig. 1A and B).

In the past, we have reported that IL4 is secreted by primary cancer cells isolated from breast cancer specimens (29) and constitutes an autocrine and paracrine prosurvival signal for breast and colorectal TICs (6, 7, 29). In ADSCs-CM, the secreted IL4 levels were comparable with those in the TN-CM and greater than in the ER^+-CM (Fig. 1A). Likewise, ER^+ MCF7 cells expressed significant lower IL4 mRNA levels than TN SUM159 established cell line (∼40-fold difference; Supplementary Fig. S1C). Of note, the exposure to ADSCs-CM, for 6 hours, boosted the IL4 mRNA levels of ER^+-BCSCs and MCF7 cells (Supplementary Fig. S1D).

Although the ER^+-BCSCs morphologic shape was not affected by the exposure to ADSCs-CM or IL4 (data not shown), TN-BCSCs acquired elongated protrusions early on, expanding in all directions (Fig. 1C). Thus, this phenomenon indicates a susceptibility of TN-BCSCs to acquire a migratory phenotype upon microenvironmental stimuli.

We also assessed the capability of breast cancer cells to expand in response to ADSCs-CM and IL4 stimuli and found a stepwise increase in the proliferation of both ER^+- and TN-BCSCs as well as bulk MCF7 and SUM159 cells (Fig. 1D and Supplementary Fig. S1E). In presence of ADSCs-CM and IL4, stem cell frequency resulted in a 2- to 3-fold increase of in ER^+- and TN-BCSCs (Fig. 1E), and was paralleled by a significant increase in the formation of colonies (Fig. 1F) large in size (>90 μm; Fig. 1G; Supplementary Fig. S1F).

ADSCs boost BCSCs proliferation and invasion in an IL4-dependent manner

To investigate whether IL4 is the main player within ADSCs-secreted cytokines that enhance the aggressiveness of breast cancer cells, we evaluated its receptor expression on ER^+- and TN-BCSCs. Both BCSC subtypes displayed IL4Rα along with IL13Rα2, a receptor inhibitor of IL13 signaling (Supplementary Fig. S2A and S2B; ref. 30).

Accordingly, we interfered with IL4 ligand/receptor interaction by using an IL4Rα antagonist, which consists of a double mutant IL4 (IL4DM) generated by the replacement of two amino acids (R121D and Y124D; refs. 24, 31). This molecule binds to IL4Rα and IL13Rα1 with the same affinity as the wild-type IL4 but lacks the agonistic activity (Supplementary Fig. S2C). Because the *in vitro* exposure to IL4DM for 72 hours impaired the proliferation of ER^+- and TN-BCSCs, MCF7, and SUM159 cells (Fig. 2A; Supplementary Fig. S2D), we sought to explore whether IL4 targeting was necessary and sufficient to limit the effect of the ADSCs-CM.

Both ADSCs-CM and IL4 strongly increased the formation of colonies in the 3D culture (Fig. 2B), which highlights that the effect of other paracrine cytokines, including IL13, is only partial. IL4DM was not only able to affect the ability to form colonies (Fig. 2B), but also to impair the invasive potential of ER^+- and TN-BCSCs and of the established cell lines MCF7 and SUM159, which counteracted the effect of both IL4 and ADSCs-CM (Fig. 2C; Supplementary Fig. S2E).

We found that BCSCs, pretreated with medium or IL4 and subcutaneously injected into mice, delayed the tumor outgrowth when IL4DM was intraperitoneally administered (Fig. 2D; ref. 6). These findings suggest that IL4DM delays the *in vivo* growth rate of BCSCs.

IL4DM inhibits MAPK pathway activation, upregulates DUSP4 expression, and sensitizes to anticancer therapy

We wondered whether the administration of IL4DM could be implicated in the modification of the $CD44^+/CD24^-$ phenotype of breast TICs with a mesenchymal-like state (16). In TN-BCSCs, CD24 expression increased in response to IL4DM, suggesting that tumor cells with stem-like features may transit between a mesenchymal-like and a less aggressive epithelial-like phenotype (Fig. 3A; Supplementary Fig. S3A; refs. 9, 32). We did not notice any significant change in CD24 expression in the exiguous compartment of $CD24^-$ cell fraction present in the ER^+-BCSCs, following exposure to IL4DM (data not shown).

It has recently been demonstrated that the depletion of $CD44^+/CD24^-$ population is determined by the exogenous expression of DUSP4 (9). DUSP4 is highly expressed in ER^+-BCSCs, whereas it was barely detectable in the TNBC subtype. ER^+- and TN-BCSCs, in presence of IL4DM and ADSCs-CM, gradually increased the expression of DUSP4 for up to 24 hours (Fig. 3B).

Published OnlineFirst April 11, 2017; DOI: 10.1158/0008-5472.CAN-16-3126

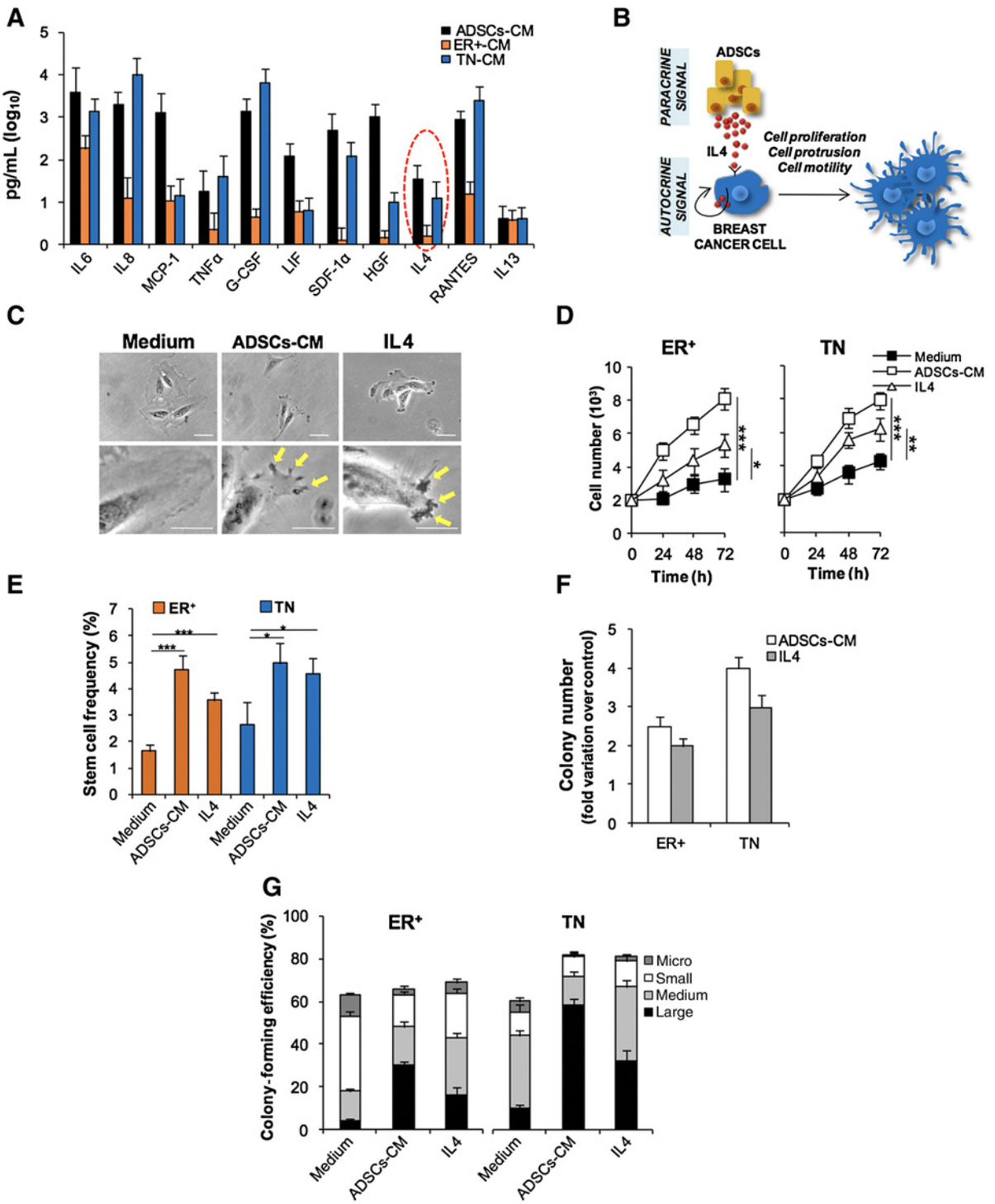

Figure 1.

ADSC-CM and IL4 enforce the motility and proliferation of BCSCs. **A,** Cytokines production of CMs derived from ADSCs, ER$^+$-BCSCs, and TN-BCSCs after 48 hours. **B,** Schematic model of paracrine and autocrine signals occurring in breast cancer cells. **C,** Representative phase contrast analysis of TN-BCSCs (pt #30) in presence of the indicated treatment and cultured in adherence for 12 hours. Arrows, cells protrusions. Scale bars, 20 μm. **D,** Cell proliferation analysis of ER$^+$-BCSCs and TN-BCSCs treated with medium, ADSCs-CM, or IL4. **E,** Stem cell frequency of ER$^+$-BCSCs and TN-BCSCs treated as in **D** at 21 days. **F,** Fold increase of colony number in ER$^+$-BCSCs and TN-BCSCs treated as in **E**. **G,** Colony-forming efficiency of cells treated as indicated. Data are expressed as mean ± SD of three independent experiments using two different ER$^+$-BCSC (pt #4 and pt #18) and two TN-BCSC (pt #10 and pt #30) lines. *, $P < 0.05$; **, $P < 0.01$; ***, $P < 0.001$.

Published OnlineFirst April 11, 2017; DOI: 10.1158/0008-5472.CAN-16-3126

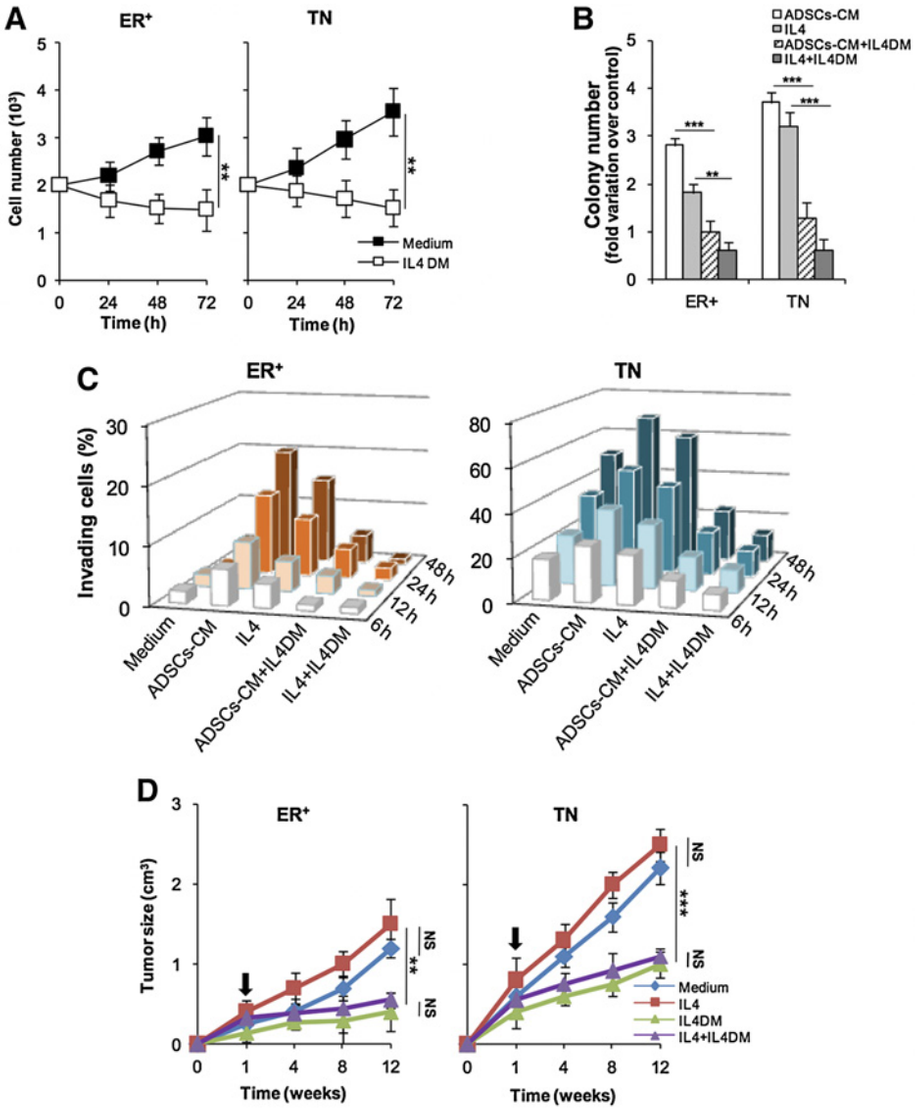

Figure 2.
IL4 promotes an invasive and tumorigenic activity in BCSCs. **A,** Cell proliferation of ER$^+$-BCSCs and TN-BCSCs treated with medium or IL4DM up to 72 hours. **B,** Fold increase of ER$^+$-BCSCs and TN-BCSCs colony number treated with medium alone (medium), ADSCs-CM, IL4, ADSCs-CM in combination with IL4DM, or IL4+IL4DM. **C,** Percentage of invading BCSCs pretreated with IL4DM for 24 hours and subsequently exposed to ADSCs-CM or IL4 for another 48 hours. After the treatment, cells were monitored for their invasive capacity up to 48 hours. Data represented in figures are mean ± SD of three independent experiments using two different ER$^+$-BCSCs (pt #4 and pt #18) and two TN-BCSCs (pt #10 and pt #30). **D,** Size of tumors generated by subcutaneous injection of 4×10^3 ER$^+$-BCSCs or TN-BCSCs pretreated with medium or IL4 for 24 hours. Mice were then treated intraperitoneally with vehicle or IL4DM from week 1 (arrows) to week 11. Mice were monitored up to 12 weeks. Data are mean ± SD of two subcutaneously injected BCSC lines for each molecular subtype ($n = 4$ mice per condition indicated). **, $P < 0.01$; ***, $P < 0.001$; NS, nonsignificant.

It was reported that the MAPK pathway activity, including in breast cancer, is partially modulated by DUSP4 (9–12). We hypothesized that the effect of IL4DM in impairing proliferation and invasive potential of BCSCs could be due to the DUSP4-mediated downregulation of MAPK pathway. IL4DM decreased the activity of MEK, ERK, and RAS, at 45 minutes and 24 hours (Fig. 3C), even in presence of ADSCs-CM and IL4 in both ER$^+$- and TN-BCSCs (Fig. 3D and E; Supplementary Fig. S3B–S3D). In ER$^+$-BCSCs, which retain high levels of DUSP4, IL4DM slightly augmented its levels in the absence or presence of ADSCs-CM or IL4 (Fig. 3C–E). Similarly, IL4DM prompted DUSP4 expression in MCF7 and SUM159 cells (Supplementary Fig. S3E). Although IL4DM boosted DUSP4 expression in TN-BCSCs (Fig. 3C), this effect was weaker in presence of IL4 and ADSCs-CM (Fig. 3D and E; Supplementary Fig. S3B–S3D). NF-κB has been reported to be modulated by IL4 treatment in B lymphocytes (33) and to promote the expansion of breast TICs, which contribute to cancer progression (34, 35). To understand how the IL4 signaling blockade is capable of modulating expression levels of DUSP4, we analyzed the activation of NF-κB. The phosphorylation of NF-κB was enhanced by IL4 exposure of both ER$^+$- and TN-BCSCs, whereas its expression levels were barely present in ER$^+$-BCSCs and potently lowered in TN-BCSCs by the addiction of IL4DM to the cell culture (Fig. 3F; Supplementary Fig. S3F). Withaferin A (Wit A), which selectively inhibits IKKβ (36, 37), overcame the effects of IL4, reducing the NF-κB activation to a greater extent in TN-BCSCs (Fig. 3G; Supplementary Fig. S3G). Wit A restored in ER$^+$- and upregulated in TN-BCSCs the DUSP4 expression levels in the presence of IL4 (Fig. 3H). 5-Aminosalicylic acid (5-ASA), another NF-κB inhibitor (38), behaved like Wit A in boosting the expression of DUSP4 in both ER$^+$- and TN-BCSCs (Supplementary Fig. S3H).

Because IL4 blockade circumvents the resistance to conventional antitumor treatment (6, 7), we aimed to couple the inhibition of IL4 with conventional therapies used in breast cancer management. In this context, several clinical trials are evaluating the effectiveness of standard therapy in combination with PI3K

Published OnlineFirst April 11, 2017; DOI: 10.1158/0008-5472.CAN-16-3126

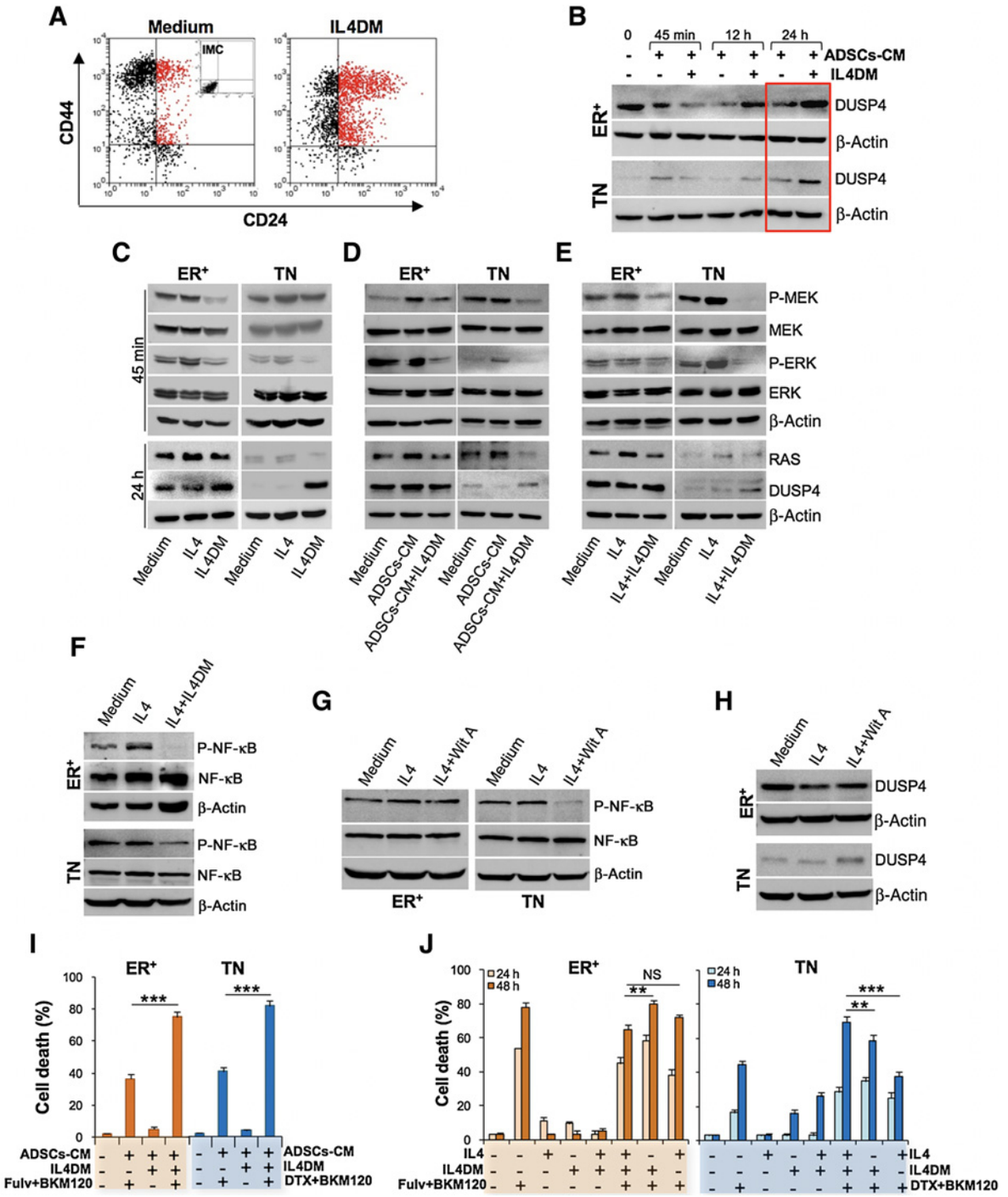

Figure 3.

IL4DM prevents the activation of MAPK pathway. **A,** Representative flow cytometry analysis of IMC, CD44, and CD24 on TN-BCSCs (pt #30) treated as indicated for 72 hours. Red dots, double positive cells. **B,** Immunoblot analysis for DUSP4 of ER$^+$-BCSCs (pt #18) and TN-BCSCs (pt #30) treated as shown at the indicated time points. Red box, the time point selected for the further experiments. β-Actin was used as loading control. **C–E,** Western blot analysis for P-MEK, MEK, P-ERK, ERK at 45 minutes and for RAS and DUSP4 at 24 hours of ER$^+$-BCSCs (pt #18) and TN-BCSCs (pt #30) exposed to the indicated treatment. β-Actin was used as loading control. **F.** Immunoblot analysis for P-NF-κB and NF-κB of ER$^+$-BCSCs (pt #18) and TN-BCSCs (pt #30) treated with the indicated agents for 45 minutes. β-Actin was used as loading control. **G,** Western blot analysis for P-NF-κB and NF-κB of cells treated as indicated for 45 minutes. **H,** Immunoblot analysis for DUSP4 of cells as in **G** exposed to the indicated treatment for 24 hours. **I,** Percentage of cell death in cells exposed to ADSCs-CM in combination with IL4DM and Fulvestrant+BKM120 (Fulv+BKM120) for ER$^+$-BCSCs or Docetaxel+BKM120 (DTX+BKM120) for TN-BCSCs at 48 hours. **J,** Cell death percentage of cells exposed to IL4 in combination with IL4DM and treated with antitumoral drugs as in **I** at the indicated time points. Bars represent mean ± SD of three independent experiments performed with two ER$^+$-BCSC (pt #4 and pt #18) and two TN-BCSC (pt #10 and pt #30) lines. *, $P < 0.05$; ***, $P < 0.001$; NS, nonsignificant.

Published OnlineFirst April 11, 2017; DOI: 10.1158/0008-5472.CAN-16-3126

inhibitors, such as BKM120, in both ERα-negative and -positive breast cancers (39, 40).

IL4DM in combination with BKM120 and the ERα inhibitor, fulvestrant (Fulv), for ER^+-BCSCs, or the chemotherapeutic compound docetaxel (DTX), for TNBC subtype, in presence of microenvironmental cytokines present in the ADSCs-CM, significantly potentiated cell death induced by treatment alone in both ER^+- and TN-BCSCs, reaching from 40% to 80% (Fig. 3I).

To determine the specific contribution of IL4 in mediating the refractoriness to therapy, we exposed BCSCs to the combination of IL4DM with the indicated anticancer compounds in presence of IL4. Although ER^+-BCSCs exposed to fulvestrant plus BKM120 (Fulv+BKM120) did not benefit from the addition to the treatment of IL4DM (Fig. 3J), the latter significantly increased the efficacy of docetaxel plus BKM120 (DTX+BKM120) in TN-BCSCs at both 24 and 48 hours in the presence or absence of IL4 (Fig. 3J). These data suggest that the inhibition of IL4 achieves only a partial response in ER^+-BCSC model due to their extreme sensitivity to fulvestrant and BKM120, whereas enhances drug efficacy in TNBC model.

DUSP4 reduces proliferation, invasion, and metastatic potential of BCSCs

To assess the role of DUSP4 with regard to tumorigenic and metastatic potential, we stably knocked-down DUSP4 (shDUSP4) in ER^+-BCSCs and MCF7 cells and ectopically expressed it (DUSP4) in TN-BCSCs and SUM159 cells (Fig. 4A; Supplementary Fig. S4A–S4C). shDUSP4 provoked a slight increase in ER^+-BCSC proliferation, which was delayed in TN-BCSCs overexpressing DUSP4 (Fig. 4B). The analysis of the invasion assay revealed a potent capability of ER^+-BCSCs harboring shDUSP4 to invade the Matrigel in response to the chemoattractant human serum AB. The ectopic expression of DUSP4 curtailed the invasive potential of TN-BCSCs (Fig. 4C). Moreover, the knockdown of DUSP4 led to an enrichment in cells able to form large colonies, whereas their reduction was dictated by DUSP4 ectopic expression (Fig. 4D).

In accordance with already published data, DUSP4 knockdown, in ER^+-BCSCs, increased the $CD44^+/CD24^-/CD90^-$ compartment, conversely TN-BCSCs, ectopically overexpressing DUSP4, showed a significant decrease of this cell fraction (Fig. 4E; Supplementary Fig. S4D and S4E) by the modulation of MAPK pathway activation (Fig. 4F; Supplementary Fig. S4F; ref. 9). Likewise, shDUSP4 in MCF7 cells and DUSP4 overexpression in SUM159 cells, respectively, enhanced or decreased the activation of MEK, ERK, and P38 MAPKs (Supplementary Fig. S4G).

By modulating EMT effectors and molecules, which control breast cancer invasion, P38 has been implicated in multiple steps of the metastatic process (41). Thus, we reasoned that DUSP4 could be involved in the metastatic dissemination of BCSCs. *In vivo* imaging analysis of cells transduced with luciferase showed that shDUSP4 rendered ER^+-BCSCs able to colonize the liver and the lung when injected in the tail vein of NOD/SCID mice (Fig. 4G). Conversely, TN-BCSCs overexpressing DUSP4 lost their metastatic potential (Fig. 4H). Collectively, these findings confirm the tumor suppressor role of DUSP4 and unveil a novel role in inhibiting metastasis.

IL4 favors a more permissive microenvironment

We subsequently evaluated the clinical relevance of IL4 and DUSP4 in breast cancer patients by interrogating a publically available database (PROGgeneV2—Pan Cancer Prognostics Database-GSE10893-GPL887). High expression of IL4 and low expression levels of DUSP4 resulted to be associated with a decreased relapse-free survival of patients affected by breast cancer (HR 2.36; 95% CI, 1.15–4.85; $P = 0.019$; Fig. 5A). IL4 biological main function relies on the modulation of immune response (42). We investigated whether adipose tissue, aided by the infiltrating T lymphocytes, could foster a protumorigenic microenvironment. Tumor cells escape from the cytotoxic activity of $CD8^+$ cells through the expression of PD-L1, which by binding to its receptor, PD-1, promotes the apoptosis of cytotoxic T cells (43). IL4DM markedly diminished the expression of PD-1 on the surface of activated cytotoxic $CD8^+$ T cells, as compared with its control (medium) and regardless of the presence of IL4 (Fig. 5B; Supplementary Fig. S5A and S5B). We found that the treatment with IL4 reduced the percentage (of about 15% vs. medium) of activated cytotoxic $CD8^+$ T cells expressing IFNγ. Although IL4DM alone did not alter T-cell activation, it was notably able to counteract the effect of IL4, restoring the number of cytotoxic T cells expressing IFNγ (Fig. 5C; Supplementary Fig. S5B). As ER^+- and TN-BCSCs express PD-L1 (Supplementary Fig. S5C), we hypothesize that IL4DM could potentially limit the activation of the PD-1 pathway by reducing the number of cytotoxic PD-1/$CD8^+$ T-cell compartment. These phenomena suggest the existence of a negative DUSP4 feedback loop that inhibits the MAPK pathway, as well as the production of cytokines involved in the priming of microenvironment that fuels cancer progression (Fig. 5D).

Discussion

Here, we provided evidence that BCSCs with a metastatic propensity express high levels of IL4 along with a downregulation of DUSP4. The latter is confirmed by the inverse correlation between relapse-free survival of breast cancer patients and IL4 expression. Targeting inflammatory mediators in breast cancer has pointed out appealing endpoints *in vitro* and in preclinical models (31, 44). Notwithstanding the ongoing development of innovative therapeutic agents that block inflammatory cytokines released by tumor microenvironment and involved in the progression of breast cancer, nowadays the clinical use of these therapies does not show improvement in patient outcome (45). On the basis of our previous findings in colorectal cancer (6), we here investigated the IL4-mediated mechanism that regulates the tumorigenic and metastatic potential of BCSCs.

Targeting IL4 signaling depleted the tumorigenic and metastatic $CD44^+/CD24^-$ cell fraction, thus delaying the proliferation and invasion capability of BCSCs through the inhibition of MEK, ERK, and RAS activity. Notably, ER^+-BCSCs expressed elevated levels of IL4Rα and were promoted to produce IL4 following microenvironmental cytokine stimuli, although to a lesser extent than TN-BCSCs. Our data indicated that nonmetastatic ER^+-BCSCs, under tumor microenvironmental influence, acquire an invasive phenotype by strengthening IL4 signaling activity, which is overcome by the blockade of IL4Rα with IL4DM.

We observed that blocking IL4 signaling, by IL4DM, increases the expression of DUSP4 concomitantly with the downregulation of RAS–MAPK pathway. It has recently been demonstrated that in physiologic conditions, the activation of MAPK promotes DUSP4 expression, which in turn suppresses ERK, ensuring breast cell

Published OnlineFirst April 11, 2017; DOI: 10.1158/0008-5472.CAN-16-3126

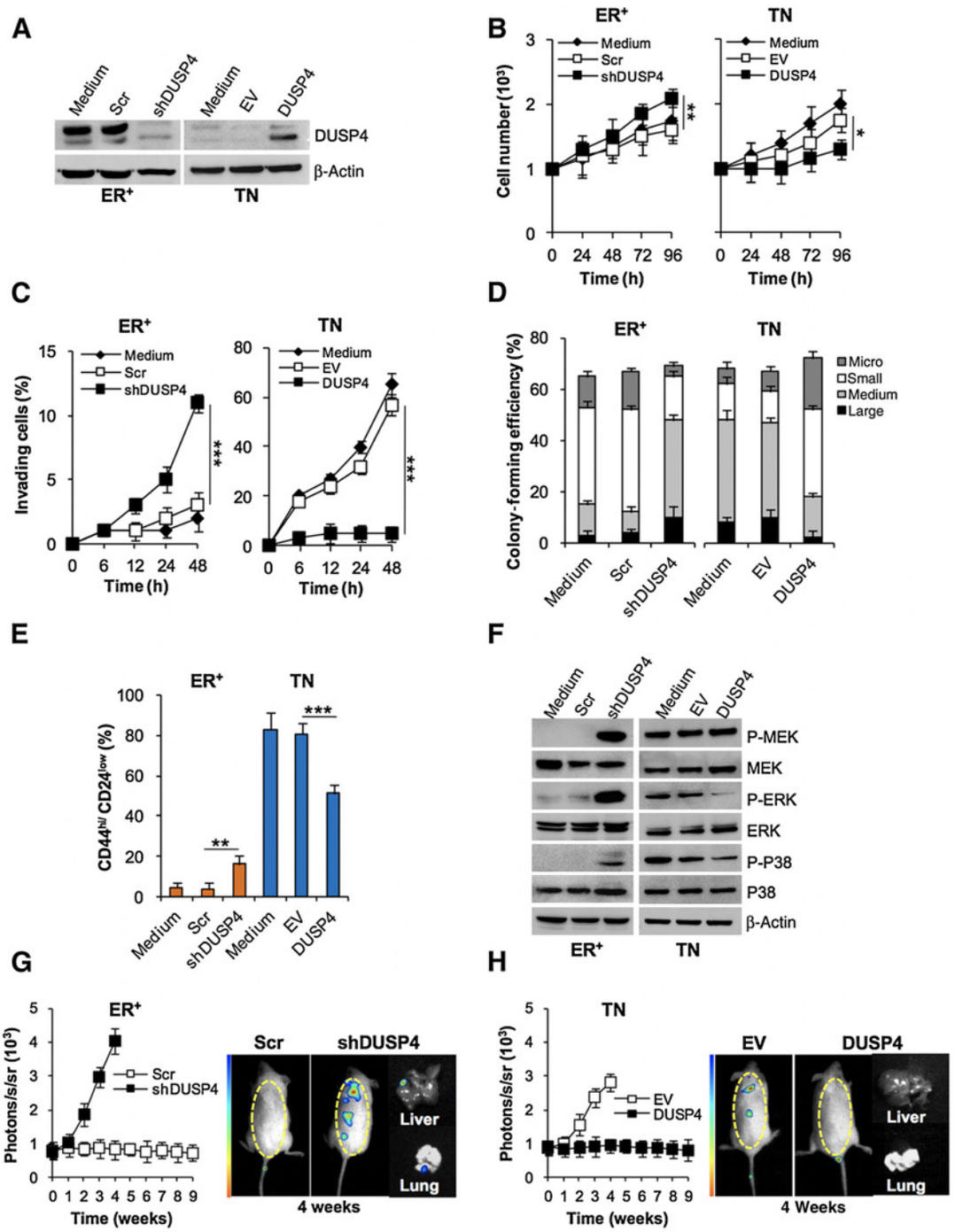

Figure 4.

DUSP4 hampers the metastatic potential of BCSCs. **A,** Western blot analysis for DUSP4 of ER$^+$- BCSCs (pt #18) exposed to medium alone and transduced with scramble (Scr) and short hairpin DUSP4 (shDUSP4) and TN-BCSCs (pt #30) transduced with empty vector (EV) and DUSP4 synthetic gene (DUSP4). β-Actin was used as loading control. **B,** Cell proliferation of cells transduced as in **A**. **C,** Percentage of invading cells as described in **A**. **D,** Percentage of colony forming efficiency of cells as in **A**. **E,** Percentage of CD44^{high}/CD24^{low} positivity of cells treated as in **A** by flow cytometry analysis. Data are expressed as mean ± SD of three independent experiments using two different ER$^+$-BCSC (pt #4 and pt #18) and two TN-BCSC (pt #10 and pt #30) lines. **F,** Immunoblot analysis of P-MEK, MEK, P-ERK, ERK, P-P38, P38 of cells transduced as in **A**. β-Actin was used as loading control. **G** and **H,** *In vivo* whole-body imaging analysis of mice tail vein injected with cells transduced with scramble (Scr) and shDUSP4 (shDUSP4) for ER$^+$-BCSCs and with empty vector (EV) and DUSP4 synthetic gene (DUSP4) for TN-BCSCs. Yellow dashed ellipse outlines the area of metastasis used for photons count. Data shown are mean ± SD of two BCSC lines for each molecular subtype injected into the tail vein of three mice for each indicated condition. *, $P < 0.05$; **, $P < 0.01$; ***, $P < 0.001$.

Published OnlineFirst April 11, 2017; DOI: 10.1158/0008-5472.CAN-16-3126

turnover. Nevertheless, loss of DUSP4 and its methylation lead to an aberrant cell proliferation in basal-like breast cancers (9, 10). In addition, the activation of NF-κB signaling plays a crucial role in downregulating the expression levels of DUSP4 in endothelial cells (46). Strikingly, our data revealed that DUSP4 is inhibited by NF-κB activation in an IL4-dependent manner.

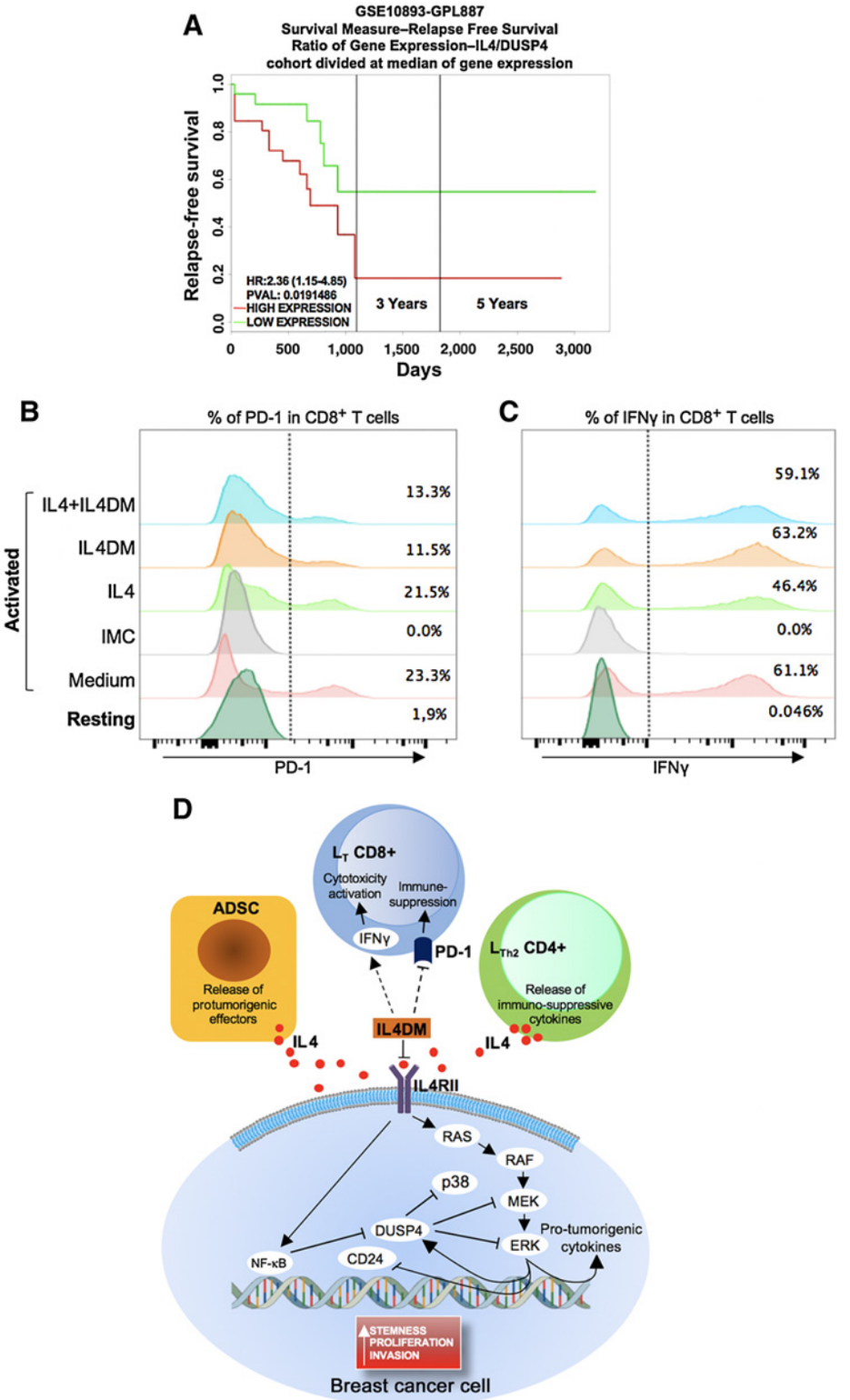

Figure 5.
IL4 contributes to the protumorigenic microenvironment. **A,** Relapse-free survival Kaplan–Meier curves according to IL4/DUSP4 gene expression ratio in breast cancer patients. **B,** Flow cytometry analysis of PD-1 and its IMC on PBMCs gated for CD8 positivity ($CD8^+$ T cells). Activated PBMCs (Activated) refers to cells exposed to anti-CD3 in combination with anti-CD28 mAbs for 4 days. Activated cells were then treated, for additional 4 days, with medium (medium), IL4 (IL4), IL4DM (IL4DM), or IL4 in combination with IL4DM (IL4+IL4DM). Resting PBMCs (Resting) represent nonactivated cells cultured in presence of medium alone. **C,** Representative flow cytometry analysis of IFNγ on resting and activated $CD8^+$ T cells treated as in **B**. **D,** Schematic model illustrating IL4 signaling in breast cancer cells. ADSCs and $CD4^+$ T helper type 2 lymphocytes (L_{Th2}) secrete IL4 into the tumor microenvironment. IL4 binding to its cognate receptor, IL4RII, on breast cancer cells triggers the activation of RAS–MAPK pathway, which promotes cancer stemness and is in turn blocked by DUSP4. Concurrently, IL4-mediated NF-κB activation cooperates in the blockage of DUSP4. Antagonizing IL4Rα, with IL4DM, inhibits IL4 signaling in cancer cells and favors cytotoxic $CD8^+$ L_T activation.

Published OnlineFirst April 11, 2017; DOI: 10.1158/0008-5472.CAN-16-3126

Compelling data indicate that P38 and ERK activation promotes cancer cell dormancy, allowing their survival in a hostile microenvironment. In addition, P38 induces EMT awakening cancer cells from dormancy (41, 47). The overexpression of DUSP4 potently impaired ERK and P38 MAPK pathway, preventing the intrinsic metastatic capability of BCSCs.

Within tumor microenvironment, aside from ADSCs, infiltrating $CD4^+$ T_{h2} lymphocytes are the other main source of IL4 (42). IL4 mediates the switching of $CD4^+$ T_{h1} cells to $CD4^+$ T_{h2} cells affecting their innate antitumor immunity (42). Although the activation of IL4/STAT6 signal boosts both the tumorigenic and metastatic activity of breast cancer cells, its loss exerts an antitumor activity through the activation of $CD8^+$ T cells, in a $CD4^+$ L_{Th} cell-independent manner (19, 48). Although the role of T_{h2} cytokines in cancer is still contradictory and context dependent (49), we here demonstrated that targeting IL4 pathway fostered the cytotoxicity of $CD8^+$ T cells, by increasing intracellular IFNγ content and decreasing their PD-1 expression, expression that is related with a shorter overall survival in epithelial-originated cancer patients (50).

Finally, our findings propose the targeting of IL4 signaling as a powerful approach in reducing tumor burden and metastatic colonization. Several commercially available compounds that block IL4 signaling are presently being utilized in the treatment of asthma and some have already been tested in clinical trials as anticancer agents (8). Their administration, in combination with other novel more effective therapies such as MEK, ERK, and PI3K inhibitors, warrants further investigation to establish their effective doses and efficacy.

Disclosure of Potential Conflicts of Interest

No potential conflicts of interest were disclosed.

Authors' Contributions

Conception and design: M. Gaggianesi, A. Turdo, S. Vieni, G. Stassi, M. Todaro
Development of methodology: M. Gaggianesi, A. Turdo, A. Chinnici, E. Lipari, I. Sperduti, E. Lo Presti, S. Vieni
Acquisition of data (provided animals, acquired and managed patients, provided facilities, etc.): T. Apuzzo, A. Benfante, S. Di Franco, V. Caputo, S. Vieni
Analysis and interpretation of data (e.g., statistical analysis, biostatistics, computational analysis): A. Chinnici, E. Lipari, T. Apuzzo, A. Benfante, I. Sperduti, S. Di Franco, S. Meraviglia, E. Lo Presti, G. Militello
Writing, review, and/or revision of the manuscript: M. Gaggianesi, A. Turdo, I. Sperduti, F. Dieli, S. Vieni, G. Stassi, M. Todaro
Study supervision: M. Todaro

Acknowledgments

The authors thank Prof. Max Wicha for kindly providing SUM159 cell line and Apogenix GmbH, Heidelberg for supplying IL4DM. We thank Francesco Calò for his help on the graphic images, Alessandro Gorgone and Giovanni Tomaselli for their technical assistance, Tatiana Terranova for editing the manuscript, Emanuela Scavo for STR genotyping analysis, Alessandro Giammona for providing assistance in experiments involving ADSCs-CM. A. Turdo and S. Di Franco are recipients of an Associazione Italiana per la Ricerca sul Cancro (AIRC) fellowship. A. Chinnici is a PhD student of molecular and experimental medicine PhD programme at University of Palermo in partnership with Humanitas University.

Grant Support

This work was supported by grants from Associazione Italiana per la Ricerca sul Cancro (AIRC) 14415 to M. Todaro and AIRC 16746 to G. Stassi.

The costs of publication of this article were defrayed in part by the payment of page charges. This article must therefore be hereby marked *advertisement* in accordance with 18 U.S.C. Section 1734 solely to indicate this fact.

Received November 23, 2016; revised March 2, 2017; accepted April 7, 2017; published OnlineFirst April 11, 2017.

References

1. Arnedos M, Vicier C, Loi S, Lefebvre C, Michiels S, Bonnefoi H, et al. Precision medicine for metastatic breast cancer—limitations and solutions. Nat Rev Clin Oncol 2015;12:693–704.
2. Wang YY, Lehuede C, Laurent V, Dirat B, Dauvillier S, Bochet L, et al. Adipose tissue and breast epithelial cells: a dangerous dynamic duo in breast cancer. Cancer Lett 2012;324:142–51.
3. Sinicrope FA, Dannenberg AJ. Obesity and breast cancer prognosis: weight of the evidence. J Clin Oncol 2011;29:4–7.
4. Laurent V, Guerard A, Mazerolles C, Le Gonidec S, Toulet A, Nieto L, et al. Periprostatic adipocytes act as a driving force for prostate cancer progression in obesity. Nat Commun 2016;7:10230.
5. Iyengar NM, Hudis CA, Dannenberg AJ. Obesity and inflammation: new insights into breast cancer development and progression. Am Soc Clin Oncol Educ Book 2013:46–51.
6. Todaro M, Alea MP, Di Stefano AB, Cammareri P, Vermeulen L, Iovino F, et al. Colon cancer stem cells dictate tumor growth and resist cell death by production of interleukin-4. Cell Stem Cell 2007;1:389–402.
7. Francipane MG, Alea MP, Lombardo Y, Todaro M, Medema JP, Stassi G. Crucial role of interleukin-4 in the survival of colon cancer stem cells. Cancer Res 2008;68:4022–5.
8. Bankaitis KV, Fingleton B. Targeting IL4/IL4R for the treatment of epithelial cancer metastasis. Clin Exp Metastasis 2015;32:847–56.
9. Balko JM, Schwarz LJ, Bhola NE, Kurupi R, Owens P, Miller TW, et al. Activation of MAPK pathways due to DUSP4 loss promotes cancer stem cell-like phenotypes in basal-like breast cancer. Cancer Res 2013;73:6346–58.
10. Mazumdar A, Poage GM, Shepherd J, Tsimelzon A, Hartman ZC, Den Hollander P, et al. Analysis of phosphatases in ER-negative breast cancers identifies DUSP4 as a critical regulator of growth and invasion. Breast Cancer Res Treat 2016;158:441–54.
11. Cagnol S, Rivard N. Oncogenic KRAS and BRAF activation of the MEK/ERK signaling pathway promotes expression of dual-specificity phosphatase 4 (DUSP4/MKP2) resulting in nuclear ERK1/2 inhibition. Oncogene 2013;32:564–76.
12. Hijiya N, Tsukamoto Y, Nakada C, Tung Nguyen L, Kai T, Matsuura K, et al. Genomic Loss of DUSP4 contributes to the progression of intraepithelial neoplasm of pancreas to invasive carcinoma. Cancer Res 2016;76:2612–25.
13. Zhou BB, Zhang H, Damelin M, Geles KG, Grindley JC, Dirks PB. Tumour-initiating cells: challenges and opportunities for anticancer drug discovery. Nat Rev Drug Discov 2009;8:806–23.
14. Zeuner A, Todaro M, Stassi G, De Maria R. Colorectal cancer stem cells: from the crypt to the clinic. Cell Stem Cell 2014;15:692–705.
15. Valent P, Bonnet D, De Maria R, Lapidot T, Copland M, Melo JV, et al. Cancer stem cell definitions and terminology: the devil is in the details. Nat Rev Cancer 2012;12:767–75.
16. Al-Hajj M, Wicha MS, Benito-Hernandez A, Morrison SJ, Clarke MF. Prospective identification of tumorigenic breast cancer cells. Proc Natl Acad Sci U S A 2003;100:3983–8.
17. Korkaya H, Kim GI, Davis A, Malik F, Henry NL, Ithimakin S, et al. Activation of an IL6 inflammatory loop mediates trastuzumab resistance in HER2+ breast cancer by expanding the cancer stem cell population. Mol Cell 2012;47:570–84.
18. Saha S, Mukherjee S, Khan P, Kajal K, Mazumdar M, Manna A, et al. Aspirin suppresses the acquisition of chemoresistance in breast cancer by disrupting an NF-κB-IL6 signaling axis responsible for the generation of cancer stem cells. Cancer Res 2016;76:2000–12.
19. Venmar KT, Carter KJ, Hwang DG, Dozier EA, Fingleton B. IL4 receptor ILR4α regulates metastatic colonization by mammary tumors through multiple signaling pathways. Cancer Res 2014;74:4329–40.

20. Schnitt SJ.Classification and prognosis of invasive breast cancer: from morphology to molecular taxonomy. Mod Pathol 2010;23: S60–4.
21. Todaro M, Gaggianesi M, Catalano V, Benfante A, Iovino F, Biffoni M, et al. CD44v6 is a marker of constitutive and reprogrammed cancer stem cells driving colon cancer metastasis. Cell Stem Cell 2014;14:342–56.
22. Di Franco S, Turdo A, Benfante A, Colorito ML, Gaggianesi M, Apuzzo T, et al. DeltaNp63 drives metastasis in breast cancer cells via PI3K/CD44v6 axis. Oncotarget 2016;7:54157–73.
23. Hu Y, Smyth GK. ELDA: extreme limiting dilution analysis for comparing depleted and enriched populations in stem cell and other assays. J Immunol Methods 2009;347:70–8.
24. Zurawski SM, Vega F Jr, Huyghe B, Zurawski G. Receptors for interleukin-13 and interleukin-4 are complex and share a novel component that functions in signal transduction. EMBO J 1993;12:2663–70.
25. Picon-Ruiz M, Pan C, Drews-Elger K, Jang K, Besser AH, Zhao D, et al. Interactions between adipocytes and breast cancer cells stimulate cytokine production and drive Src/Sox2/miR-302b-mediated malignant progression. Cancer Res 2016;76:491–504.
26. Gilbert CA, Slingerland JM. Cytokines, obesity, and cancer: new insights on mechanisms linking obesity to cancer risk and progression. Annu Rev Med 2013;64:45–57.
27. Walter M, Liang S, Ghosh S, Hornsby PJ, Li R. Interleukin 6 secreted from adipose stromal cells promotes migration and invasion of breast cancer cells. Oncogene 2009;28:2745–55.
28. Devarajan E, Song YH, Krishnappa S, Alt E. Epithelial-mesenchymal transition in breast cancer lines is mediated through PDGF-D released by tissue-resident stem cells. Int J Cancer 2012;131:1023–31.
29. Todaro M, Lombardo Y, Francipane MG, Alea MP, Cammareri P, Iovino F, et al. Apoptosis resistance in epithelial tumors is mediated by tumor-cell-derived interleukin-4. Cell Death Differ 2008;15:762–72.
30. Rahaman SO, Sharma P, Harbor PC, Aman MJ, Vogelbaum MA, Haque SJ. IL-13R(α)2, a decoy receptor for IL-13 acts as an inhibitor of IL-4-dependent signal transduction in glioblastoma cells. Cancer Res 2002;62:1103–9.
31. Andrews AL, Holloway JW, Holgate ST, Davies DE. IL-4 receptor α is an important modulator of IL-4 and IL-13 receptor binding: implications for the development of therapeutic targets. J Immunol 2006;176:7456–61.
32. Liu S, Cong Y, Wang D, Sun Y, Deng L, Liu Y, et al. Breast cancer stem cells transition between epithelial and mesenchymal states reflective of their normal counterparts. Stem Cell Rep 2014;2:78–91.
33. Thieu VT, Nguyen ET, McCarthy BP, Bruns HA, Kapur R, Chang CH, et al. IL-4-stimulated NF-κB activity is required for Stat6 DNA binding. J Leukocyte Biol 2007;82:370–9.
34. Kendellen MF, Bradford JW, Lawrence CL, Clark KS, Baldwin AS. Canonical and non-canonical NF-κB signaling promotes breast cancer tumor-initiating cells. Oncogene 2014;33:1297–305.
35. Biswas DK, Shi Q, Baily S, Strickland I, Ghosh S, Pardee AB, et al. NF-κ B activation in human breast cancer specimens and its role in cell proliferation and apoptosis. Proc Natl Acad Sci U S A 2004;101:10137–42.
36. Kaileh M, Vanden Berghe W, Heyerick A, Horion J, Piette J, Libert C, et al. Withaferin a strongly elicits IκB kinase β hyperphosphorylation concomitant with potent inhibition of its kinase activity. J Biol Chem 2007; 282:4253–64.
37. Heyninck K, Lahtela-Kakkonen M, Van der Veken P, Haegeman G, Vanden Berghe W. Withaferin A inhibits NF-κB activation by targeting cysteine 179 in IKKβ. Biochem Pharmacol 2014;91:501–9.
38. Egan LJ, Mays DC, Huntoon CJ, Bell MP, Pike MG, Sandborn WJ, et al. Inhibition of interleukin-1-stimulated NF-κB RelA/p65 phosphorylation by mesalamine is accompanied by decreased transcriptional activity. J Biol Chem 1999;274:26448–53.
39. Wallin JJ, Guan J, Prior WW, Lee LB, Berry L, Belmont LD, et al. GDC-0941, a novel class I selective PI3K inhibitor, enhances the efficacy of docetaxel in human breast cancer models by increasing cell death in vitro and in vivo. Clin Cancer Res 2012;18:3901–11.
40. Yamamoto-Ibusuki M, Arnedos M, Andre F. Targeted therapies for ER+/HER2- metastatic breast cancer. BMC Med 2015;13:137.
41. del Barco Barrantes I, Nebreda AR. Roles of p38 MAPKs in invasion and metastasis. Biochem Soc Transact 2012;40:79–84.
42. Kacha AK, Fallarino F, Markiewicz MA, Gajewski TF. Cutting edge: spontaneous rejection of poorly immunogenic P1.HTR tumors by Stat6-deficient mice. J Immunol 2000;165:6024–8.
43. Chen L, Han X. Anti-PD-1/PD-L1 therapy of human cancer: past, present, and future. J Clin Invest 2015;125:3384–91.
44. Ginestier C, Liu S, Diebel ME, Korkaya H, Luo M, Brown M, et al. CXCR1 blockade selectively targets human breast cancer stem cells in vitro and in xenografts. J Clin Invest 2010;120:485–97.
45. Crusz SM, Balkwill FR. Inflammation and cancer: advances and new agents. Nat Rev Clin Oncol 2015;12:584–96.
46. Kao DD, Oldebeken SR, Rai A, Lubos E, Leopold JA, Loscalzo J, et al. Tumor necrosis factor-α-mediated suppression of dual-specificity phosphatase 4: crosstalk between NF-κB and MAPK regulates endothelial cell survival. Mol Cell Biochem 2013;382:153–62.
47. Sosa MS, Avivar-Valderas A, Bragado P, Wen HC, Aguirre-Ghiso JA. ERK1/2 and p38α/β signaling in tumor cell quiescence: opportunities to control dormant residual disease. Clin Cancer Res 2011;17:5850–7.
48. Ostrand-Rosenberg S, Grusby MJ, Clements VK. Cutting edge: STAT6-deficient mice have enhanced tumor immunity to primary and metastatic mammary carcinoma. J Immunol 2000;165:6015–9.
49. Yu P, Fu YX. Tumor-infiltrating T lymphocytes: friends or foes? Lab Invest 2006;86:231–45.
50. Zhang Y, Kang S, Shen J, He J, Jiang L, Wang W, et al. Prognostic significance of programmed cell death 1 (PD-1) or PD-1 ligand 1 (PD-L1) Expression in epithelial-originated cancer: a meta-analysis. Medicine 2015;94:e515.

Published OnlineFirst April 11, 2017; DOI: 10.1158/0008-5472.CAN-16-3126

Cancer Research
The Journal of Cancer Research (1916–1930) | The American Journal of Cancer (1931–1940)

AACR American Association for Cancer Research

IL4 Primes the Dynamics of Breast Cancer Progression via DUSP4 Inhibition

Miriam Gaggianesi, Alice Turdo, Aurora Chinnici, et al.

Cancer Res 2017;77:3268-3279. Published OnlineFirst April 11, 2017.